Coupled Channel Interactions in $J/\psi \rightarrow V[PP]_{S-wave}$

John Weinstein

University of Tennessee, Knoxville, TN, 37996-1200

Abstract

We review the model which lead us to the concept of the $K\bar{K}$ Molecule and show how it can be extended to apply to S-wave pseudoscalar-pseudoscalar production spectra such as those seen in $J/\psi \rightarrow V[PP]_{S-wave}$. We present some preliminary results of this analysis.

Introduction

What is the ground state of a system composed of two quarks and two antiquarks? Our investigation of this question in the NRQM (non-relativistic quark model) concluded that it is either two free mesons or a weakly bound pseudoscalar-pseudoscalar (PP) meson system. [1,2)]

In order for two mesons to bind it is clear that the quarks in one must interact with the quarks in the other. Two color octet mesons are a linear combination of color singlet mesons in each of the two possible non-orthogonal $(q\bar{q})_1(q\bar{q})_1$ configurations,

$$(q_1\bar{q}_3)_8 \cdot (q_2\bar{q}_4)_8 = \sqrt{9/8}\,(q_1\bar{q}_4)_1\,(q_2\bar{q}_3)_1 - \sqrt{1/8}\,(q_1\bar{q}_3)_1\,(q_2\bar{q}_4)_1\,, \tag{1}$$

so the binding cannot come from the color-electric confinement potential alone.

Our analysis of the ground state $qq\bar{q}\bar{q}$ wavefunction obtained from the NRQM via the variational technique shows that one important source of meson-meson interactions is quark exchange, as pictured in Figure 1(a). In the model these processes are driven by the one gluon exchange hyperfine interaction and wavefunction symmetries. They can, of course, change the flavor structure of the PP system from the initial to the final state. In particular, consider an $ns\bar{n}\bar{s}$ system (where $n = u$ or d). Quark exchange will take a $K\bar{K}$ system into the $\eta\eta$, $\eta\eta'$, $\eta'\eta'$ system in I=0 or into the $\pi\eta$, $\pi\eta'$ system in I=1, where the physical η and η' flavor wavefunctions are taken to be

$$\eta = \frac{1}{\sqrt{2}}\left(\frac{1}{\sqrt{2}}(u\bar{u} + d\bar{d}) - s\bar{s}\right) \tag{2a}$$

$$\eta' = \frac{1}{\sqrt{2}}\left(\frac{1}{\sqrt{2}}(u\bar{u} + d\bar{d}) + s\bar{s}\right). \tag{2b}$$

Thus two quark exchange diagrams plus $\eta - \eta'$ mixing can carry one from $K\bar{K}$ to $\pi\pi$ without OZI violations.

The second important source of meson-meson interactions are via $q\bar{q}$ annihilations into the broad s-channel $^3\mathrm{P}_0$ $q\bar{q}$ resonances, the I=1 a_0 or the I=0 f_0 and f_0', and their subsequent decays as shown in Figure 1(b).[3] These diagrams also lead to PP flavor changing between initial and final states.

From these basic considerations it is clear that one cannot study a particular PP system in isolation; the meson-meson ground state is a coupled channel problem. To examine it we use the coupled channel Schrödinger equation

$$(\mathbf{K} + \mathbf{M} + \mathbf{V})\,\mathbf{u}(r) = E\,\mathbf{u}(r) \tag{3}$$

where

$$\mathbf{K}_{ij} = \frac{1}{2\mu_i}\,p_i^2\,\delta_{ij} \tag{4}$$

is the diagonal $n \times n$ non-relativistic kinetic energy matrix,

$$\mathbf{M}_{ij} = (m_1 + m_2)_i\,\delta_{ij} \tag{5}$$

is the sum of the pseudoscalar meson masses in the PP channels or the quark masses in the $^3\mathrm{P}_0$ channels,

$$\mathbf{V}_{ij} = \begin{pmatrix} \mathbf{V}\,(\mathrm{PP} \leftrightarrow \mathrm{PP}) & \mathbf{V}\,(\mathrm{PP} \leftrightarrow {}^3\mathrm{P}_0) \\ \mathbf{V}^{\mathrm{T}}\,(\mathrm{PP} \leftrightarrow {}^3\mathrm{P}_0) & \mathbf{V}\,({}^3\mathrm{P}_0 \leftrightarrow {}^3\mathrm{P}_0) \end{pmatrix}_{ij} \tag{6}$$

is a matrix representing the interactions and is discussed below, and E is the non-relativistic invariant mass. The radial wavefunctions are one of

$$\mathbf{u}^{\mathrm{I}=0} = \begin{pmatrix} \mathrm{u}_{\pi\pi} \\ \mathrm{u}_{K\bar{K}} \\ \mathrm{u}_{\eta\eta} \\ \mathrm{u}_{\eta\eta'} \\ \mathrm{u}_{\eta'\eta'} \\ \mathrm{u}_{f_0} \\ \mathrm{u}_{f_0'} \end{pmatrix}, \tag{7a}$$

$$\mathbf{u}^{\mathrm{I}=1} = \begin{pmatrix} \mathrm{u}_{\pi\eta} \\ \mathrm{u}_{K\bar{K}} \\ \mathrm{u}_{\pi\eta'} \\ \mathrm{u}_{a_0} \end{pmatrix}, \tag{7b}$$

or

$$\mathbf{u}^{\mathrm{I}=2} = (\,\mathrm{u}_{\pi\pi}\,), \tag{7c}$$

according to the isospin of interest.

The components of $\mathbf{V}\,(\mathrm{PP} \leftrightarrow \mathrm{PP})$ are square well approximations to the $(\mathrm{PP})_i \leftrightarrow (\mathrm{PP})_j$ potentials which are generated by the quark exchange mechanism of Figure 1(a). We describe their extraction from the quark model in References 1 and 2. The components of $\mathbf{V}\,(\mathrm{PP} \leftrightarrow {}^3\mathrm{P}_0)$ allow for the $q\bar{q}$ annihilations of Figure 1(b) and are represented by square well potentials with depth

$$\mathbf{V}\,(\mathrm{PP} \leftrightarrow {}^3\mathrm{P}_0)_{ij} = \mathrm{Clebsch}\,[(\mathrm{PP})_i \leftrightarrow ({}^3\mathrm{P}_0)_j]\ \sqrt{\mu_{K\bar{K}}/\mu_i}\ \Omega \tag{8}$$

and the same range as the $\mathbf{V}\,(\mathrm{PP} \leftrightarrow \mathrm{PP})$ potentials. The kinematic form factor $\sqrt{\mu_{K\bar{K}}/\mu_i}$ scales the annihilation potential by the reduced mass of the i^{th} channel relative to the $K\bar{K}$ channel, which is common to both I=0 and I=1. The overall constant Ω is predicted by Kokoski and Isgur[4] and gives, in the two channel $\pi\pi \leftrightarrow f_0$ system, the predicted $f_0 \rightarrow \pi\pi$ partial width. Finally, $\mathbf{V}\,({}^3\mathrm{P}_0 \leftrightarrow {}^3\mathrm{P}_0)$ is a diagonal matrix which gives the ${}^3\mathrm{P}_0$ $q\bar{q}$ systems their uncoupled masses and consists of a square well potential with the same range as the $\mathbf{V}\,(\mathrm{PP} \leftrightarrow \mathrm{PP})$ potentials, a $-2/(2\,\mu\,r^2)$ p-wave centrifugal barrier, and confinement imposed by a large repulsive potential outside the square well. The depth of each central square well is chosen to approximately reproduce the experimental ${}^3\mathrm{P}_0$ masses; $a_0(1300)$, $f_0(1300)$, and $f_0'(1500)$. Square well potentials are used only to simplify the calculation.

With all the operators in equation (3) known, one can integrate numerically to find the radial wavefunctions $\mathbf{u}(\mathrm{r})$ at all scattering energies E. From these wavefunctions one can find the S-matrix or T-matrix in each isospin channel.

Figure 2 shows the I=2 $\pi\pi$ phase shift prediction from the model above with some experimental data.[5] As discussed in Reference 2, meson radii predictions in the non-relativistic quark model are consistently smaller than measured radii. Since the meson-meson potentials are generated by quark exchange and annihilation processes, whose range depends on meson radii, we have expanded the range of these potentials and used the I=2 data as a fit. The repulsive character of the $\pi\pi^{\mathrm{I}=2}$ phase shift is, however, a non-trivial and unambiguous success of the calculation.

In Figure 3 we show the phase shifts for elastic $\eta\pi$ and $K\bar{K}^{\mathrm{I}=1}$ scattering using the model with the expanded range. Comparing these curves directly with experiment is not possible as $\eta\pi$ elastic processes are difficult to extract. It is however, straightforward to compare the resonant behavior of $\delta_{\eta\pi}$ below $K\bar{K}$ threshold with the phase shift due to a single resonance having the canonical mass and width of the $\delta(980)$, as is done in Figure 3. The rapid fall at threshold in the elastic $K\bar{K}$ phase shift indicates the underlying effective $K\bar{K}$ potential.

In Figure 4 we show the I=0 $\pi\pi$ phase shifts generated by the model and compare them with experimental results.[6] The elastic $\pi\pi$ phase shift is in good agreement with

the data up to $\approx$ 1.5 GeV where we expect effects such as higher $^3P_0$ $q\bar{q}$ resonances, J=0 vector-vector systems, and relativistic corrections to affect our simple model. The elastic $K\bar{K}$ phase shift (not shown) drops rapidly at $K\bar{K}$ threshold, indicating the presence of a weakly $K\bar{K}$ bound state.

As has been discussed elsewhere[1,2,7] the $K\bar{K}$ interpretation of the S^* and δ leads to clarification of many issues including:

1. the observation of two "extra" scalar states is no longer a problem;
2. the masses of the $q\bar{q}$ ^{3}P and ^{1}P states lie in the interval 1.2 to 1.5 GeV where they are naïvely expected, thus obviating the need for understanding why the S^* and δ are so light;
3. the masses of the S^* and δ, just below $K\bar{K}$ threshold, are unavoidable if they are lightly bound $K\bar{K}$ states;
4. the narrow S^* and δ widths are outcomes of the $K\bar{K}$ picture (Figures 3 and 4) but an order of magnitude too narrow for the $q\bar{q}$ picture;
5. the ratios $\Gamma(S^* \to \pi\pi)/\Gamma(\delta \to \eta\pi)$ and $\Gamma(S^* \to K\bar{K})/\Gamma(S^* \to \pi\pi)$ are not in agreement with those expected for $^3P_0$ $q\bar{q}$ states but are in accord with $K\bar{K}$ predictions;
6. the $\gamma\gamma$ widths of the S^* and δ agree with the $K\bar{K}$ but not with the $q\bar{q}$ calculations;[8]
7. a naïve application of final state interactions to the decay $\iota/\eta(1440) \to K\bar{K}\pi$ leads to $K\bar{K}$ and $K\pi$ mass distributions consistent with the data;[9]
8. the effects of the repulsive I=2 $\pi\pi$ potential and the attractive I=0 $\pi\pi$ potential combine to favour the $\Delta I=\frac{1}{2}$ decay mode of the K, removing a long-standing discrepancy between theory and experiment.[10]

A Model for PP Production

The solutions of equation (3) are "scattering" solutions in the sense that one always has some initial incoming PP system which interacts via the coupled channels to form an outgoing PP system. Consider the decay $J/\psi \to \omega\pi\pi$ where there is no incoming $\pi\pi$ system. We expect, rather, that the incoming $c\bar{c}$ state annihilates to 3 or more gluons after which approximate SU(3) symmetric $q\bar{q}$ pairs are created and recouple to form outgoing mesons. Thus the PP pairs are formed "at the origin" and suffer the interactions of (3) only on their way out of the interaction region. We therefore wish to construct a solution which has only outgoing waves but which contains the same underlying dynamics as equation (3). This requires a modification of those equations.

Imagine a point source term driving one channel in equation (3):

$$(\mathbf{K} + \mathbf{M} + \mathbf{V})\,\mathbf{u}(r) = E\,\mathbf{u}(r) + \mathbf{s}\,\delta(0)\,. \tag{9}$$

Here **s** is a column vector with unity in the driven channel and zeros elsewhere. This term corresponds to a hidden channel which couples to only one of the usual channels. It is independent of the wavefunctions $\mathbf{u}(r)$ and allows us to retain those solutions which are non-zero at the origin and normally discarded on physical grounds. We can combine the inhomogeneous solutions of equation (9) with the homogeneous solutions of equation (3) to find the "production" solutions we require, *i.e.* solutions characterized by outgoing waves only.

In the one channel case, with a central square well potential, the amplitude for the outgoing wave has a magnitude equal to the "wavefunction at the origin" factor and a phase equal to the scattering phase. For the many channel problem, at energies such that only one channel is open, the amplitude of the outgoing wave has a magnitude analogous to the wavefunction at the origin enhancement and a phase equal to the scattering phase, as required by Watson's Theorem.[11] Above the threshold for two open channels the phase of each outgoing amplitude is process dependent and no longer related to the scattering phase shifts. We interpret the magnitude of the outgoing wave as the amplitude to produce that particular PP system. If we plot the square of the outgoing amplitude times the phase space factor we can, modulo an overall constant, predict the spectrum for a given process.

We now consider $J/\psi \to \phi\pi\pi$, $J/\psi \to \phi K\bar{K}$, $J/\psi \to \omega\pi\pi$, and $J/\psi \to \omega K\bar{K}$. Some interesting but poorly understood features of these reactions are the S^* seen in the $\pi\pi$ recoiling against the ϕ, and the threshold enhancements, but no S^*, in the $\pi\pi$ system recoiling against the ω.

In Figure 5(a) we show the $K\bar{K}$ invariant mass distribution expected for the reaction $J/\psi \to \phi\,(K\bar{K}) \xrightarrow{\text{CCI}} \phi\, K\bar{K}$. (The notation means that we choose **s** in equation (9) so that $K\bar{K}$ is produced at the origin and, after the coupled channel interactions, $K\bar{K}$ appears in the final state.) The spectrum is normalized to give the same number of events as the data. In Figure 5(b) we show the spectrum for the reaction $J/\psi \to \phi\,(K\bar{K}) \xrightarrow{\text{CCI}} \phi\,\pi\pi$ normalized by the $K\bar{K}$ spectrum (adjusted for the Clebsch-Gordon factors and bin sizes). The prominence of the S^* signal in the $\pi\pi$ channel is obvious and entirely a consequence of the CCI's.

Threshold enhancements in $\pi\pi$ have been around in various guises for a long time (*e.g.* the ABC effect[12] and the indeterminant mass of the $\epsilon(700)/\epsilon(900)/\epsilon(1100)$). In Figure 6(a) we show the reaction $J/\psi \to \omega\,(\pi\pi) \xrightarrow{\text{CCI}} \omega\,\pi\pi$. This curve is normalized to give the same number of $\omega\,\pi\pi$ events as the experimental data and clearly reproduces the main features including the threshold bump, due partly to an attractive $\pi\pi$ potential, and the lack of a strong S^* signal. The $\omega K\bar{K}$ spectrum in Figure 6(b) is normalized relative to the $\omega\pi\pi$ spectrum and shows a threshold effect which is consistent with the

data.

This analysis has not yet taken into account the other possible production processes recoiling against the ω: $J/\psi \to \omega(\eta\eta)$, $\to \omega(\eta\eta')$, $\to \omega(\eta'\eta')$ and $\to \omega f_0(1300)$ which will feed both the $\omega K\bar{K}$ and $\omega\pi\pi$ final states and thus modify the spectra in Figures 6. The same remarks apply to the ϕ recoil spectra of Figures 5.

Conclusions

It is clear that quark exchange interactions and PP $\leftrightarrow$ $^3P_0$ transition amplitudes have significant effects on low energy meson-meson dynamics and may provide, within the context of a simple coupled channel model, the explanation for many long standing problems with low energy spectroscopy and invariant mass distributions. More work is needed to see if these interactions alone are sufficient to understand all the observed details. High statistics J/ψ decays are clearly an important testing ground.

Other important applications are the "easy" extensions to systems such as the $K\pi$, J=2 VV, J=1 VP, and J=1 VV as well as to harder problems such as $D\bar{D}$, $\bar{K}N$, J=0 VV and unitary 3-body final state interactions.

While the coupled channel solution is perhaps not exciting, in the sense that it is based on simple physics and not on new particles or new types of interactions, it would clearly be exciting to have at last a common solution to many of the diverse puzzles mentioned here.

I would like to thank my collaborator, Nathan Isgur, as well as Ted Barnes, Frank Close and Joe Macek for helpful discussions.

References

1. J. Weinstein and N. Isgur, Phys. Rev. Lett. **48**, 659 (1982); Phys. Rev. **D27**, 588 (1983).
2. J. Weinstein and N. Isgur, UTPT-89-03/UTK-89-03, to appear in PR**D**.
3. We are grateful to V.J. Pandaripande for emphasizing the possible importance of this coupling to us.
4. R. Kokoski and N. Isgur, Phys. Rev. **D35**, 907 (1987).
5. A compilation by F. Wagner in Proceedings of the XVII Int. Conf. on High Energy Physics, London, 1974 (Rutherford Lab, Chilton, Didcot, England, 1974), p. II-27 and the data of J. Prukop *et al.*, Phys. Rev. **D10**, 2055 (1974).
6. G. Grayer *et al.*, Nucl. Phys. **B75**, 189 (1974).
7. J. Weinstein, Proc. of the BNL Workshop on Glueballs, Hybrids, and Exotic Hadrons, 1988 .
8. T. Barnes, Phys. Lett. **165B**, 434 (1985).
9. M. Frank, N. Isgur, P. O'Donnell, J. Weinstein, Phys. Lett. **158B**, 442, (1985); Phys. Rev. **D32**, 2971 (1985).
10. N. Isgur, K. Maltman, J. Weinstein, T. Barnes, UTPT-89-10.
11. K.M. Watson , Phys. Rev. **89**, 575 (1953).
12. N. Booth and A. Abashian, Phys. Rev. **132**, 2314 (1963) and references therein.

(a) (b)

Figure 1. Meson-meson interactions via (a) quark exchange diagrams and (b) $q\bar{q}$ annihilation and creation through broad s-channel $^3P_0$ mesons.

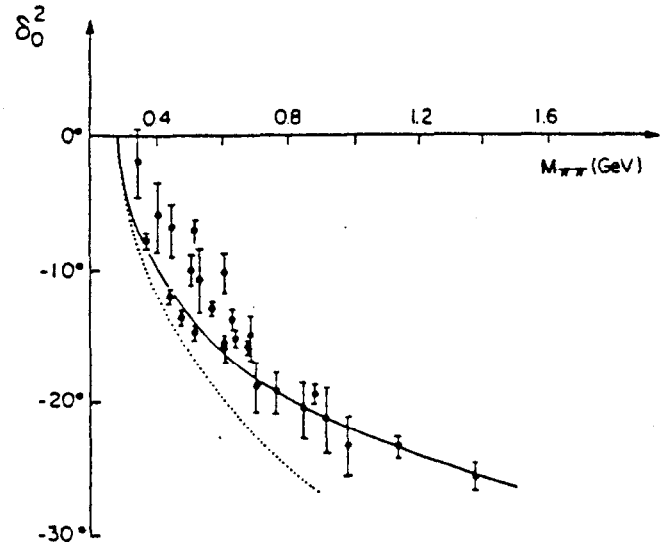

Figure 2. The I=2 $\pi\pi$ phase shift data from Reference 5 with the phase shift from the range-expanded model. The dotted curve is the phase shift with the same potential but the relativistic $\pi\pi$ energy and shows that relativistic effects could be absorbed by a slightly different rescaling of the potentials.

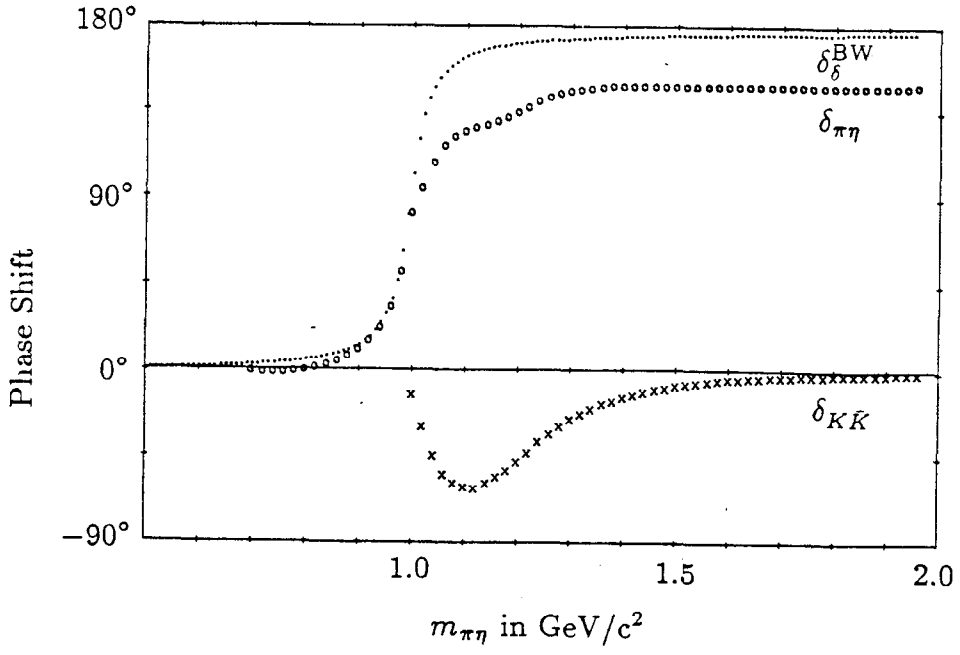

Figure 3. The elastic I=1 $K\bar{K}$ and $\pi\eta$ phase shifts (x's and o's respectively) from the model shown with the Breit-Wigner phase shift from a resonance with the parameters of the $\delta(980)$ (dots).

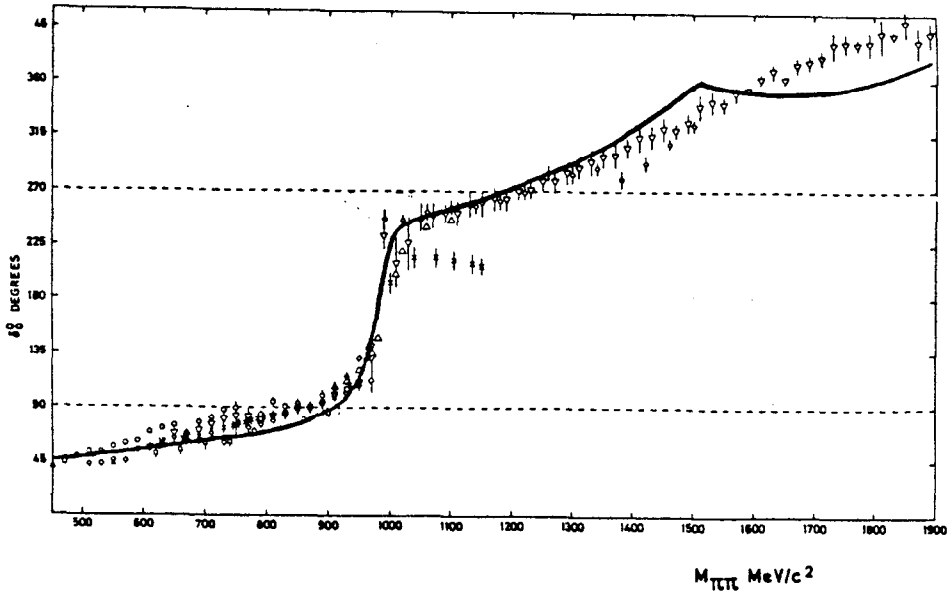

Figure 4. The I=0 $\pi\pi$ phase shift data from Reference 6 and the phase shift generated by the model.

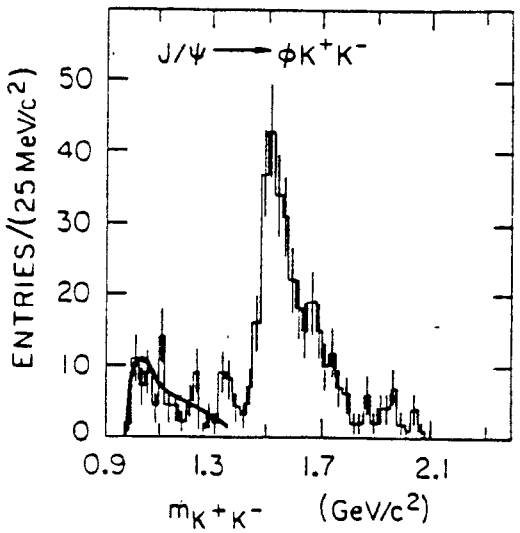

(a) $J/\psi \to \phi(K\bar{K}) \xrightarrow{\text{CCI}} \phi K\bar{K}$

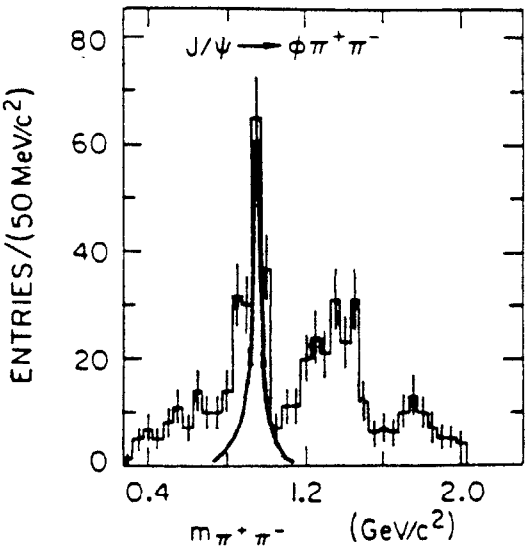

(b) $J/\psi \to \phi(K\bar{K}) \xrightarrow{\text{CCI}} \phi\pi\pi$

Figure 5. $J/\psi \to \phi(\mathrm{PP})$. The smooth curves on the data are the predictions of the model. (a) is used to normalize (b).

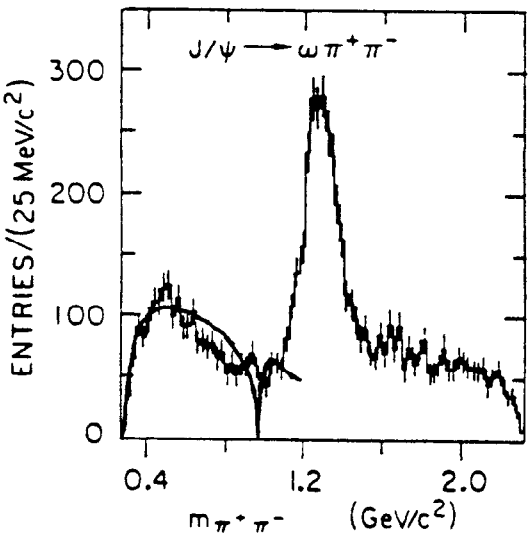

(a) $J/\psi \to \omega(\pi\pi) \xrightarrow{\text{CCI}} \omega\pi\pi$

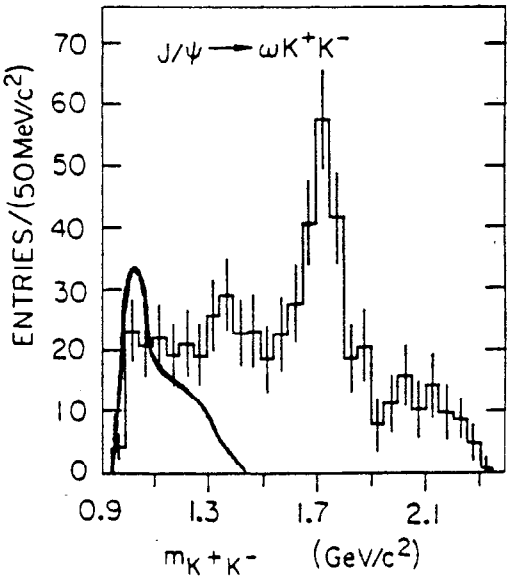

(b) $J/\psi \to \omega(\pi\pi) \xrightarrow{\text{CCI}} \omega K\bar{K}$

Figure 6. $J/\psi \to \omega(\mathrm{PP})$. The smooth curves on the data are from the model. (a) is used to normalize (b).